Vibrational Spectroscopy of Intermediates in Methane-to-Methanol Conversion by FeO^+

Gokhan Altinay, Murat Citir and Ricardo B. Metz

Supporting Information

Reference#33 from paper:

1. Frisch, M. J.; Trucks, G. W.; Schlegel, H. B.; Scuseria, G. E.; Robb, M. A.; Cheeseman, J. R.; Montgomery Jr., J. A.; Vreven, T.; Kudin, K. N.; Burant, J. C.; Millam, J. M.; Iyengar, S. S.; Tomasi, J.; Barone, V.; Mennucci, B.; Cossi, M.; Scalmani, G.; Rega, N.; Petersson, G. A.; Nakatsuji, H.; M.Hada; Ehara, M.; Toyota, K.; Fukuda, R.; Hasegawa, J.; Ishida, M.; Nakajima, T.; Honda, Y.; Kitao, O.; Nakai, H.; Klene, M.; Li, X.; Knox, J. E.; Hratchian, H. P.; Cross, J. B.; Adamo, C.; Jaramillo, J.; Gomperts, R.; Stratmann, R. E.; Yazyev, O.; Austin, A. J.; Cammi, R.; Pomelli, C.; Ochterski, J. W.; Ayala, P. Y.; Morokuma, K.; Voth, G. A.; Salvador, P.; Dannenberg, J. J.; Zakrzewski, V. G.; Dapprich, S.; Daniels, A. D.; Strain, M. C.; Farkas, O.; Malick, D. K.; Rabuck, A. D.; Raghavachari, K.; Foresman, J. B.; Ortiz, J. V.; Cui, Q.; Baboul, A. G.; Clifford, S.; Cioslowski, J.; Stefanov, B. B.; Liu, G.; Liashenko, A.; Piskorz, P.; Komaromi, I.; Martin, R. L.; Fox, D. J.; Keith, T.; Al-Laham, M. A.; Peng, C. Y.; Nanayakkara, A.; Challacombe, M.; Gill, P. M. W.; Johnson, B.; Chen, W.; Wong, M. W.; Gonzalez, C.; Pople, J. A. *Gaussian 03*, Gaussian, Inc.: Pittsburgh PA, Wallingford CT, 2004.

	CCSD(T)/6-311+G(d,p)		CCSD(T)/6-311+G(3df,p)	
Species	Quartet	Sextet	Quartet	Sextet
$FeO^+ + CH_4$	50	0	45	0
$OFe^+(CH_4)$	-51	-92	-63	-99
TS1	34	59	12	60
$[HO\text{-}Fe\text{-}CH_3]^+$	-139	-153	-153	-159
TS2	-30	-9	-44	-16
$Fe^+(CH_3OH)$	-185	-174	-197	-210
$Fe^+ + CH_3OH$	-21	-54	-31	-49

Table S1. Calculated CCSD(T)/6-311+G(d,p) and CCSD(T)/6-311+G(3df,p) energies of stationary points for the $FeO^+ + CH_4 \rightarrow Fe^+ + CH_3OH$ reaction. All energies are at the B3LYP/6-311+G(d,p) geometry and include zero-point energy at B3LYP/6-311+G(d,p). Energies are in kJ/mol.

	B3LYP/SDD+;aug-cc-pVTZ
$[HO\text{-}Fe\text{-}CH_3]^+$- Ar sextet	28.1
$[HO\text{-}Fe\text{-}CH_3]^+$- Ar quartet	36.6
$[HO\text{-}Fe\text{-}CH_3]^+$Ar-Ar sextet	19.3
$[HO\text{-}Fe\text{-}CH_3]^+$Ar-Ar quartet	11.7
$Fe^+(CH_3OH)$-Ar sextet	5.9
$Fe^+(CH_3OH)$-Ar quartet	42.3

Table S2. Calculated argon binding energies. All energies are at the B3LYP level, with the SDD basis set on Fe and aug-cc-pVTZ on remaining atoms and include zero-point energy at the same level of theory. All energies are 0 Kelvin values, in kJ/mol.

	r(O-H) Å	r(C-H) Å	r(Fe-C) Å	r(Fe-O) Å	r(C-O) Å	Θ(O-Fe-C) degrees
CH_3OH	0.961	1.088 1.094 1.094	-	-	1.423	-
$[HO\text{-}Fe\text{-}CH_3]^+$ sextet	0.966	1.092 1.091 1.091	1.969	1.738	-	137.7
$[HO\text{-}Fe\text{-}CH_3]^+$ quartet	0.967	1.105 1.085 1.085	1.966	1.703	-	111.1
$[HO\text{-}Fe\text{-}CH_3]^+(Ar)$ sextet	0.966	1.091 1.091 1.091	1.971	1.747	-	133.5
$[HO\text{-}Fe\text{-}CH_3]^+(Ar)$ quartet	0.966	1.093 1.089 1.083	1.989	1.706	-	105.6
$[HO\text{-}Fe\text{-}CH_3]^+(Ar)_2$ sextet	0.965	1.091 1.090 1.090	1.982	1.754	-	129.6
$[HO\text{-}Fe\text{-}CH_3]^+(Ar)_2$ quartet	0.965	1.094 1.087 1.084	1.991	1.714	-	104.3
$Fe^+(CH_3OH)$ sextet	0.968	1.086 1.086 1.085	-	2.044	1.477	-
$Fe^+(CH_3OH)$ quartet	0.965	1.086 1.086 1.084	-	1.943	1.476	-
$Fe^+(CH_3OH)(Ar)$ sextet	0.967	1.086 1.086 1.085	-	2.045	1.475	-
$Fe^+(CH_3OH)(Ar)$ quartet	0.965	1.086 1.086 1.084	-	1.941	1.472	-

Table S3. Geometries of bare and argon tagged $[HO\text{-}Fe\text{-}CH_3]^+$ and $Fe^+(CH_3OH)$ calculated at the B3LYP/SDD (on Fe);aug-cc-pVTZ (other atoms) level.

	O-H stretch	C-H stretches
$[HO\text{-}Fe\text{-}CH_3]^+$ quartet	3593***(282)***	3067***(3)***, 3000***(6)***, 2787***(37)***
$[HO\text{-}Fe\text{-}CH_3]^+$ sextet	3619***(356)***	3006***(12)***, 3000***(10)***, 2895***(54)***
$[HO\text{-}Fe\text{-}CH_3]^+$(Ar) quartet	3608***(267)***	3079***(5)***, 3002***(5)***, 2896***(27)***
$[HO\text{-}Fe\text{-}CH_3]^+$(Ar) sextet	3627***(305)***	3009***(5)***, 3000***(6)***, 2900***(40)***
$[HO\text{-}Fe\text{-}CH_3]^+(Ar)_2$ quartet	3621***(239)***	3073***(2)***, 3006***(1)***, 2895***(22)***
$[HO\text{-}Fe\text{-}CH_3]^+(Ar)_2$ sextet	3636***(275)***	3011***(3)***, 3007***(3)***, 2905***(31)***

Table S4. Harmonic vibrational frequencies for bare and argon-tagged insertion intermediates at the PBEPBE/SDD;aug-cc-pVTZ level, in cm^{-1}. IR intensities (km/mol) in parentheses. Frequencies have been scaled by 0.986.

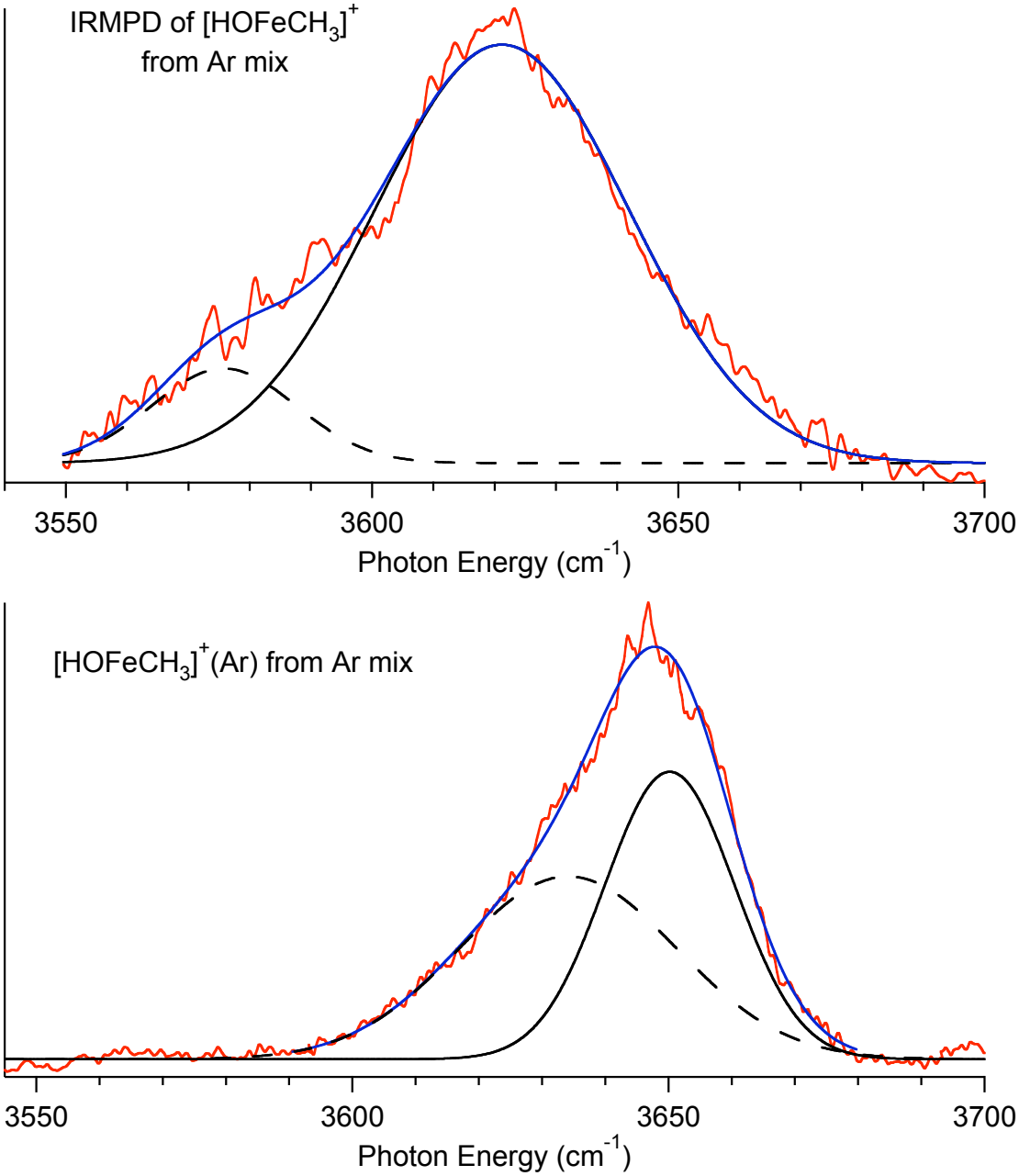

Figure S1. Spectra of $[HO\text{-}Fe\text{-}CH_3]^+$ (top) and $[HO\text{-}Fe\text{-}CH_3]^+(Ar)$ (bottom), along with fits to sum of two Gaussians and contributions from each Gaussian. Fitting parameters : peak (FWHM) in cm^{-1}:

$[HO\text{-}Fe\text{-}CH_3]^+$: 3576 (28); 3621 (49)

$[HO\text{-}Fe\text{-}CH_3]^+(Ar)$: 3632 (40); 3647 (24)

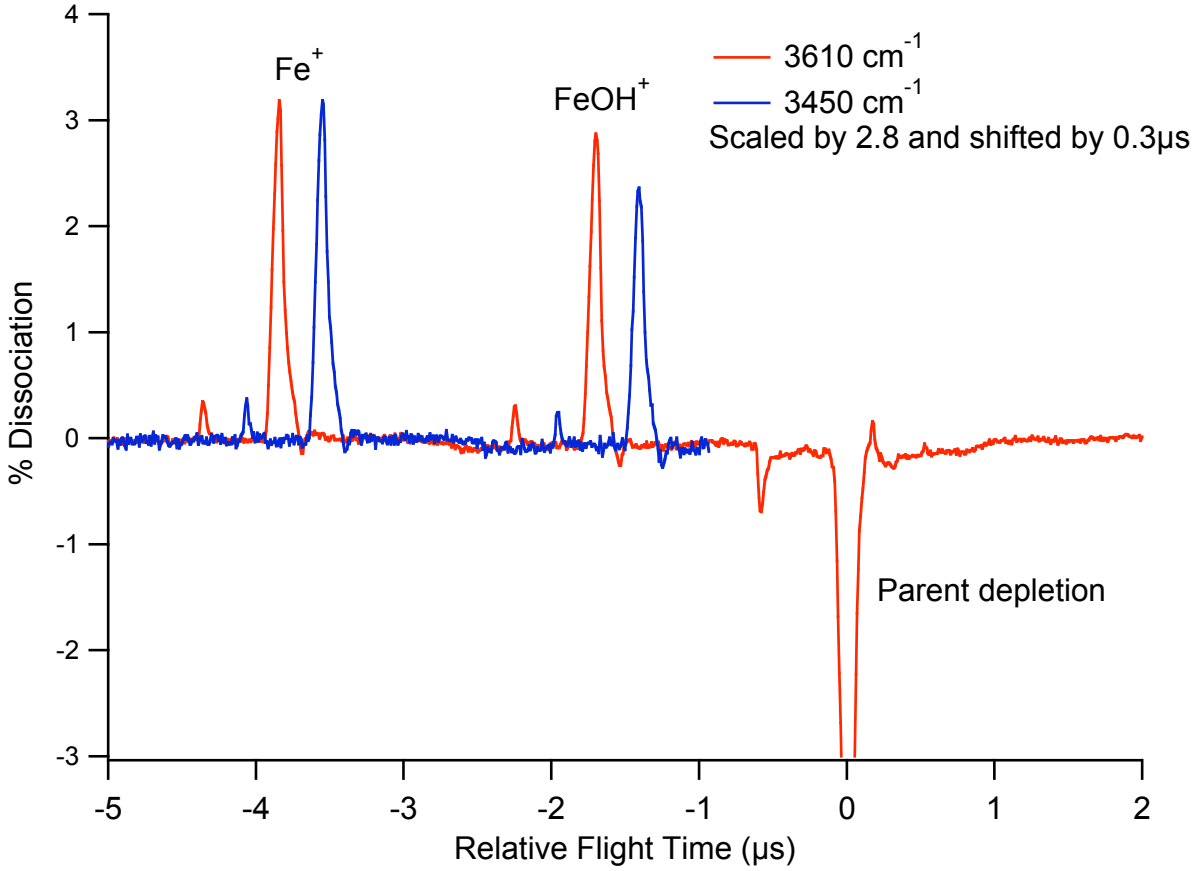

Figure S2. Difference spectra of $[FeCH_4O]^+$ from CH_3OH/90% He/10% Ar mix at 3610 cm^{-1} and 3450 cm^{-1}. The small peaks ~0.7 μs before each major peak are due to the iron-54 isotopomer.

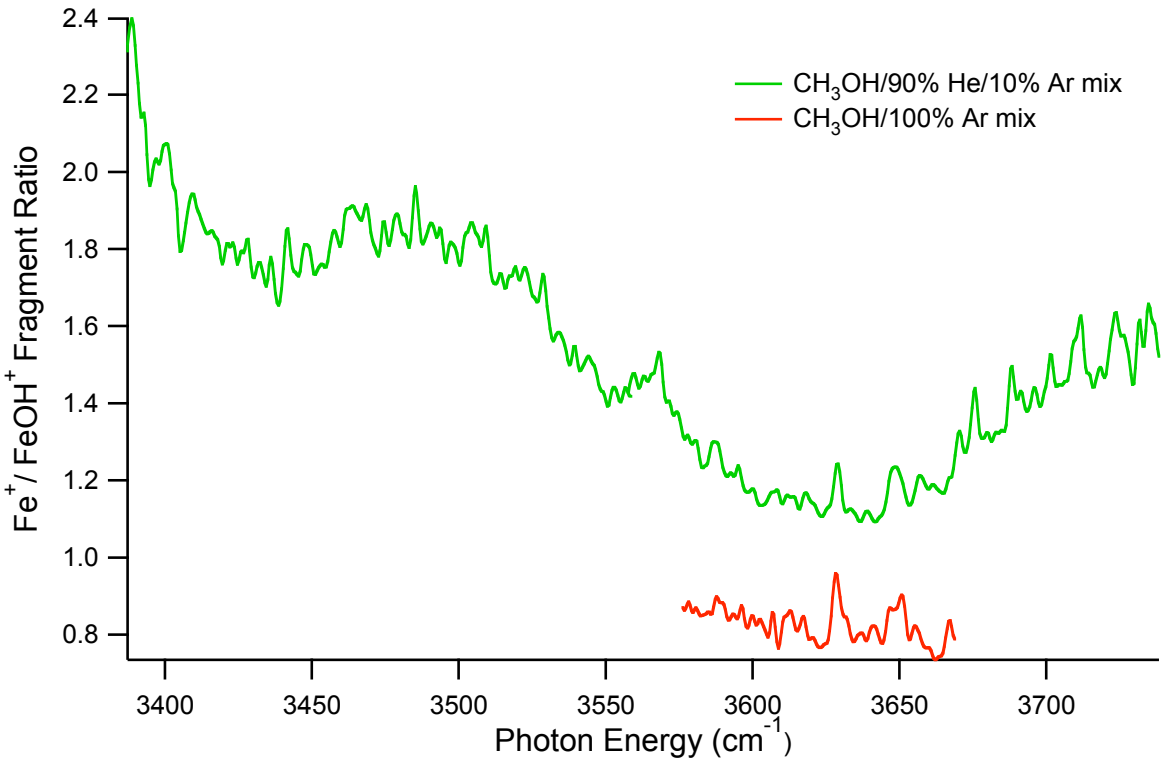

Figure S3. $Fe^+/FeOH^+$ fragment ratios from IRMPD of $[FeCH_4O]^+$ produced by reacting Fe^+ with methanol in argon (red) and 90% helium/10% argon (green). IRMPD of $Fe^+(CH_3OH)$ predominately produces Fe^+, while dissociation of $[HO\text{-}Fe\text{-}CH_3]^+$ primarily forms $FeOH^+$.